Journal of Environmental Chemical Engineering 8 (2020) 104247

Contents lists available at ScienceDirect

Journal of Environmental Chemical Engineering

journal homepage: www.elsevier.com/locate/jece

Production of microporous Cu-doped BTC (Cu-BTC) metal-organic framework composite materials, superior adsorbents for the removal of methylene blue (Basic Blue 9)

Muhammet Ş.A. Eren[a], Hasan Arslanoğlu[b,*], Harun Çiftçi[c]

[a] Izmir Institute of Technology, Faculty of Engineering, Department of Chemical Engineering, İzmir, Turkey
[b] Kırşehir Ahi Evran University, Faculty of Engineering and Architecture, Department of Chemical and Process Engineering, Kırşehir, Turkey
[c] Kırşehir Ahi Evran University, Faculty of Medicine, Department of Biochemistry, Kırşehir, Turkey

ARTICLE INFO

Editor: Teik Thye Lim

Keywords:
Cellulosic woven waste
Metal-organic framework MOF
Methylene blue (Basic Blue 9) removal
Adsorption
Desorption
Isotherm-kinetic-thermodinamic

ABSTRACT

Cellulosic woven waste was used as a biomass material to prepare a Cu-doped BTC (Cu-BTC) adsorbent, which was then used to remove methylene blue (Basic Blue 9) from wastewater. Cellulosic woven waste was used as a biomass material to prepare a Cu-doped BTC (Cu-BTC) adsorbent, which was then used to remove methylene blue (Basic Blue 9) from wastewater. The Cu-BTC had higher adsorption capacity for methylene blue (BB9) than pure woven waste because it had high specific surface area and electrostatic interaction with cationic methylene blue molecules. The Cu-BTC removed methylene blue from wastewater rapidly and effectively and had an excellent adsorption capacity (197.90 mg/g). In batch process, the adsorption efficiency of the adsorbent for removal of BB9 was evaluated within 20 °C–60 °C, with initial BB9 concentrations of 50 − 200 mg/L and initial pH of 2 − 11. The Cu-BTC activation tailored the topological and textural properties of the obtained adsorbent, leading to a relatively large surface area of 1418.3 m^2/g and pores with a volume of 0.491 cm^3/g and an average size of 2.11 nm. The adsorption process fitted well with the Langmuir isotherm and the pseudo-second-order kinetic model. The possible mechanism for methylene blue removal mainly involved electrostatic attraction and micro pores. This study can serve as a guide for value-added utilization of cellulosic woven waste and as a practical method for the removal of methylene blue from wastewater. Adsorption of methylene blue onto the Cu-BTC is an effective and eco-friendly method for its removal from wastewater.

1. Introduction

Most dyes are pollutants of high environmental impact because they are either mixed with water during production or discharged directly into water bodies by the textile, paper, and leather processing industry. For example, about 15 % of dyes is lost during the dying process in the textile industry [1]. Discharge of dyes and auxiliary chemicals into water resources causes major environmental problems because they are composed of large molecular organic compounds.

A large amount of water is used for the production of textile materials. What is more, a wide range of organic/inorganic and simple chemicals are used for the production of polymeric chemicals, resulting in wastewater containing various compositions and pollutants [2,3]. Dye effluents, even at low concentrations, are among the major water pollutants due to their increased application in the textile industry. Some dyes are carcinogenic and mutagenic, and thus, adversely affect both aquatic and human life. Discharge of dyes may cause eutrophication, oxidation, hydrolysis, and some other chemical reactions [4]. Most dyes preserve their color properties even in the presence of light, water, and chemicals [5]. Therefore, biological water treatment processes are ineffective in the treatment of dyes [6].

There are three types of methods for removing dyes from wastewater: chemical, physical, and biological. Chemical methods (photochemical degradation, electrochemical degradation, etc.) involve oxidizing agents, such as ozone, hydrogen peroxide, and sodium hypochlorite. Biological methods are conventional methods of wastewater treatment used for removing dyes from water bodies. Various methods have been developed to remove microorganisms (fungi, aerobic and anaerobic bacteria) and dyes from wastewater. Some of the physicochemical methods are adsorption, ion exchange, membrane separation, and electrokinetic separation. Of these methods, adsorption and ion exchange processes are promising physicochemical methods for water treatment. Adsorption by active carbon is the most effective method for removing dyes as well as many other contaminants from

* Corresponding author.
E-mail addresses: muhammeteren@iyte.edu.tr (M.Ş.A. Eren), hasan.arslanoglu@ahievran.edu.tr (H. Arslanoğlu), hciftci@ahievran.edu.tr (H. Çiftçi).

https://doi.org/10.1016/j.jece.2020.104247
Received 5 May 2020; Received in revised form 30 June 2020; Accepted 3 July 2020
Available online 06 July 2020

water bodies. In recent years, studies have focused on manufacturing cost-effective adsorbents from different substances or making commercially available adsorbents more cost-effective or activating them to improve their effectiveness [5,6].

Agricultural residues or by-products contain cellulose and lignin and have high adsorption capacity and are also good at retaining ionic compounds through ion exchange thanks to their acidic-basic groups. Therefore, there has recently been growing interest in agricultural waste and by-products to remove dyestuffs from industrial wastewaters [7–15]. Some of those agricultural waste and by-products are sugar cane [16], rice husk [17], rice straw [18], peanut shell [19], coconut shell [20], palm fruit seed membrane [21], cedar shavings [22], and sunflower seed husk [23]. Chemical methods have been developed to obtain adsorbents from cellulose and/or pectin-containing substances.

Metal-organic frameworks (MOFs) are one, two or three-dimensional networks constructed from inorganic salts and multidentate organic linkers. MOFs have received considerable attention in recent years because they have large surface areas and internal pore volume and the capacity to bear various functionalities. They are widely used for gas storage, adsorption/separation, and catalysis. They can be in various forms (beads, pellets, etc.), and therefore, have a low pressure drop and high performance in industrial applications. MOFs should be deposited on suitable substrates rather than encapsulating them to use their inner surface in the most effective way [24–28].

Cellulosic woven is a textile waste generally used for burning. However, based on the rationale stated above, it can also be used as an absorbent for wastewater treatment. Cotton textile waste is cellulosic. Cellulosic fibers $(C_6H_{10}O_5)_n$ prepared by the polycondensation of glucose units can be converted into MOFs. Therefore, textile manufacturers can use cellulosic fibers to treat the wastewater that they generate.

The Cu-BTC is a MOF synthesized from copper (II) nitrate and Benzene-1,3,5-tricarboxylic acid. It is widely used for catalysis, sensitivity (against specific gases), controlled release, separation, and storage. However, it is also a MOF that can be potentially used in different areas because it is positively charged, and therefore, capable of attaching to negatively charged surfaces, one of which is cellulose. Edge cut and fiber waste is a rich source of cellulose.

The aim of this study was to obtain a Cu-doped BTC (Cu-BTC) from cellulosic woven waste and to investigate its characteristics. A characterization study was conducted to investigate whether the Cu-BTC was suitable for adsorption. Based on XRD, SEM, FT-IR analyses, an experiment was performed for the adsorption of methylene blue (Basic Blue 9) in wastewater on the Cu-BTC.

2. Materials and methods

2.1. Materials preparation

The Cu-BTC obtained from cellulosic textile waste was used to remove methylene blue from wastewater, and then, its removal properties were investigated. Cellulosic textile waste (cut edges of cotton towels) was supplied from the *Saray Örme* facilities in Bursa and then cut and shredded into fibers.

Carboxymethylation was carried out for the deposition of the Cu-BTC. First, a 100 mL 15 wt % NaOH (Merck %99.9) solution (molar ratio: 2:1 ethanol (Merck, %96) / deionized water) was prepared. The cellulosic woven waste was added into the solution and stirred for 30 min, and then, was removed from the solution, into which 11.6 g of sodium chloroacetate (Merck, %99) was added. Afterwards, the cellulosic woven waste was put into the solution again and stirred for 1 h, and then, was removed from the solution and immersed into deionized water for 30 min, and then, was washed first with deionized water and then with ethanol. The cotton fabric was allowed to dry to room temperature and then dried in an oven for 1 h at 60 °C. The first step of carboxymethylation is given in Fig. 1.

Trimesic acid (1.68 g; 8 mmol) (Merck, %98) was dissolved in 100 mL ethanol:DMF (Merck, %97) (1:1 v/v) solution, which was then mixed with a 50 mL aqueous solution of 1.86 g (8 mmol) $Cu(NO_3)_2.2.5\ H_2O$ (Merck, %99.9). One gram of short cellulosic woven waste was added to the solution and stirred for about 15 min. The mixture was heated to 85 °C in a 400 mL vessel. Some of the mixture (sample 1) was kept at 85 °C for 24 h without stirring. The remaining mixture (sample 2) was stirred at 85 °C for 24 h to investigate the effect of stirring. After 24 h, both samples were separately filtered and washed with Ethanol:H_2O mixture to get rid of impurities. Afterwards, both samples were allowed to dry to room temperature for a short amount of time. Lastly, they were kept in an oven at 160 °C for 18 h to activate the fibers (Fig. 1) [27,29].

2.2. Preparation of solutions

A stock solution of Merck methylene blue (Basic Blue 9)(Merck, %99.9) was prepared at 1000 mg/L concentration. Then, some distilled water was dissolved in the solution and prepared to a volume of 1 L. Smaller concentrations of methylene blue solutions were prepared by diluting the stock solution with distilled water.

2.3. Instrumentation and characterization

The Cu-BTC composite product was characterized using SEM-EDX (SE) (scanning electron microscopy, Zeiss), TGA-DTA (FEI Quanta 250 FEG), particle size distribution (Malvern Master Sizer 3000), pH_{zpc} (Malvern Nanosize ZS-3600 zetasizer). Specific surface area, total pore volume, and adsorption average pore diameter were determined using a BET (Brunauer-Emmett-Teller, Micromeritics ASAP 2020). Functional groups were determined using a FT-IR spectrophotometer (ATR) (Perkin Elmer Spectrum 100).

2.4. Effect of solution pH

The effect of pH was analyzed in the range of 3–12 at 293 K for the adsorption. Half a gram of The Cu-BTC was added to a 100 mL methylene blue solution of 100 mg/L and shaken for 12 h. The absorbance of methylene blue in the samples was determined by spectrophotometric (Shimadzu UV-1201) method at 665 nm, the specific wavelength for methylene blue after dilution of samples with distilled water suitable for analysis. In determining the amount of methylene blue in the filtrates, a calibration graph prepared from the absorbance measurements determined in the spectrophotometer of standard methylene blue solutions at concentrations ranging from $1-5$ mg/L was used. Afterwards, the methylene blue removal rate was determined as follows :

$$\%\text{Methylene blue(BB9)Adsorption} = (C_o - C_s) \times \frac{100}{C_o} \quad (1)$$

where C_0 and C_e (mg/L) are the initial and the equilibrium of aqueous methylene blue concentration, respectively.

2.5. Effect of ionic strength

NaCl solutions with concentrations of 0.01 M to 0.1 NaCl were added to the 100 mL methylene blue solutions of 100 mg/L at 293 K to investigate the effect of ionic strength. All samples were agitated at 300 rpm for 12 h. Following reaction, the adsorption capacity at equilibrium (q_e [mg/g]) was determined as follows :

$$q = \frac{(C_o - C_s) \times V}{m} \quad (2)$$

Where V (L) is the volume of methylene blue solution; M (g) is the mass of absorbents; C_0 is the initial and the equilibrium concentration of methylene blue solution, and C_e (mg/L) is the equilibrium concentration of methylene blue solution.

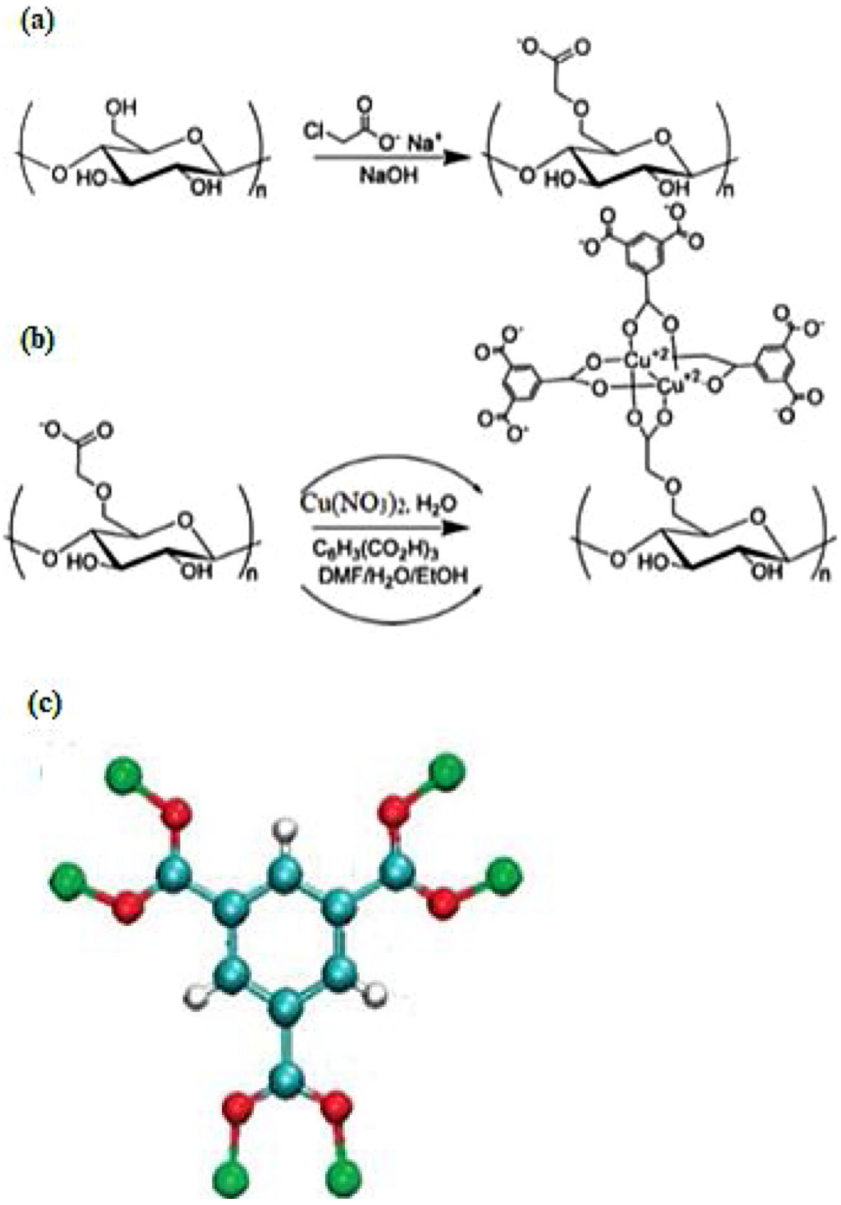

Fig. 1. Carboxymethylation of cellulosic woven waste (a), deposition process on cellulosic woven waste (b), Cu-doped BTC (Cu-BTC) (c).

Experiments were carried out in two parallel samples. The average of the two was used in the case of a deviation of < 5 percent. A third experiment was performed in the case of a deviation of > 5 percent, and the average of the two closest of these values was taken into account.

3. Result and discussion

3.1. Characterization of the Cu-BTC composite

SEM-EDX images were used to analyze the appearance and pore structure of the Cu-BTC. Fig. 2 shows that it had a cubic-like structure and a surface similar to BTC (benzene-1,3,5-tricarboxylic acid). It had an extremely dense surface with numerous small granular particles adhering to the internal pores of the composite, which might provide additional reactive sites to capture contaminants [24].

The elemental composition of the Cu-BTC was identified by the EDX spectra. The EDX spectrum shows the high purity of the synthesized Cu-BTC along with the oxygen content which indicates the formation of copper particles. The absence of other elements in the EDX spectrum also confirms the purity of the Cu-BTC as mentioned by Küsgens et al. [24].

N_2 adsorption/desorption experiments were performed to further characterize the Cu-BTC porosity. Table 1 shows the results. The Cu-BTC had a relatively high (1418.3 m^2/g) BET with a type I isotherm related to monolayer adsorption. It had a type I N_2 adsorption–desorption isotherm with an H1 type hysteresis loop characteristic of a microporous structure. This difference may be due to the introduction of Cu. This result agreed with the SEM analysis (Fig. 3) [30].

Fig. 4 shows the XRD results of the Cu-BTC, the cellulosic woven waste, and the Cu-BTC deposited cellulosic woven waste. The cellulosic woven waste had an amorphous structure (Fig. 4a). After the Cu-BTC deposition, the characteristic peaks of the Cu-BTC were observed. The peaks suggest that the Cu-BTC had a crystal structure while the cellulosic woven waste remained to be amorphous. Abdelhameed et al. [25] reported that the Cu-BTC deposited on viscose had strong MOF peaks at $2\theta = 9.4^\circ$, 11.6°, 13.4°, and 19.1° and weak peaks at $2\theta = 17.4^\circ$, 20.1°, 25.9°, 29.4°, 35.3° and 39.2°, which was similar to our results (Fig. 4b).

The Cu-BTC showed characteristic bands around 1600 cm^{-1},

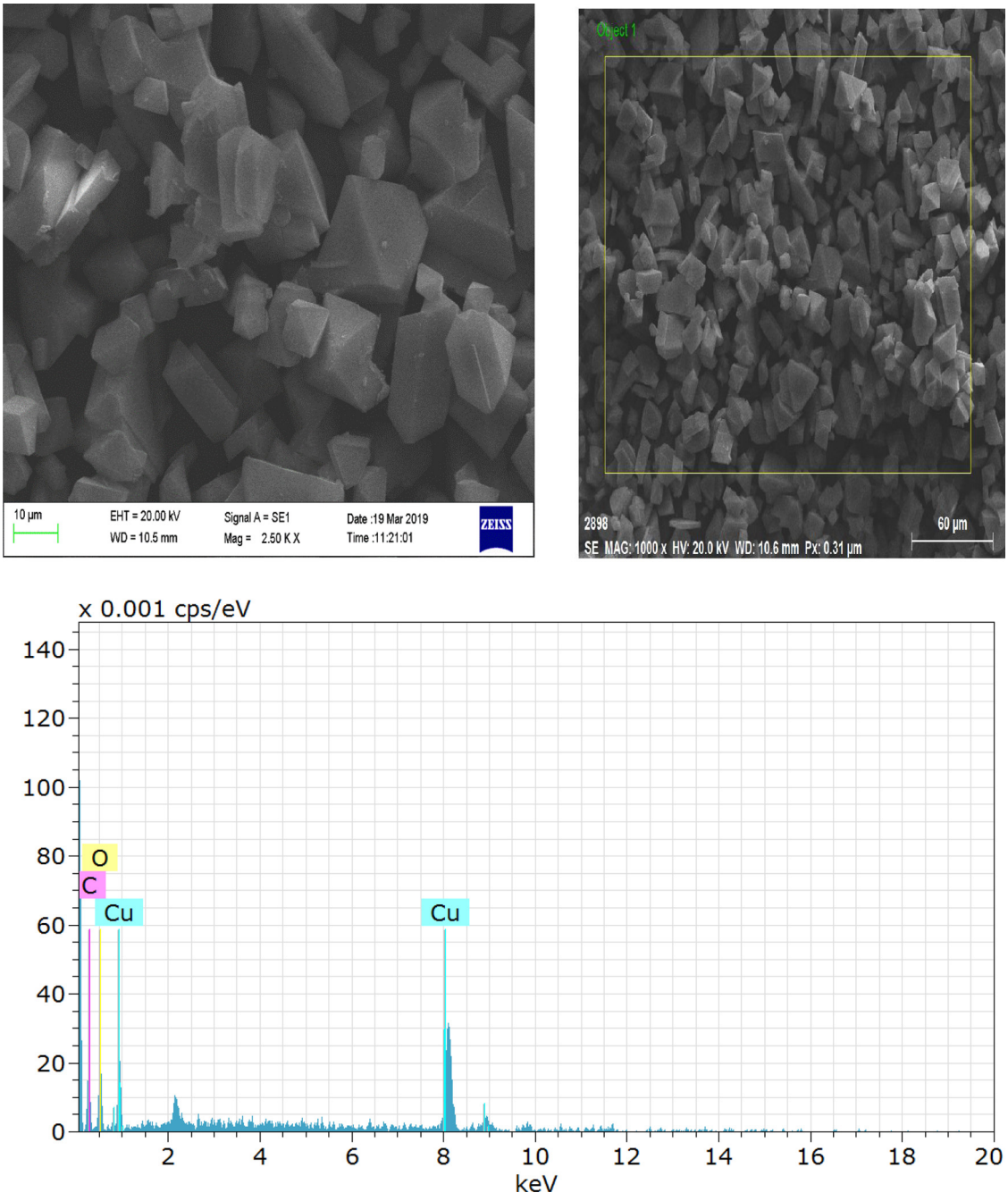

Fig. 2. SEM images of surface micromorphology of Cu-doped BTC (Cu-BTC) and EDX evaluation.

Table 1
Some chemical/physicochemical properties of Cu-doped BTC (Cu-BTC.).

Property	Value
Bulk density (g/cm^3)	0.824
True density (g/cm^3)	1.546
BET surface area (m^2/g)	1418.3
Langmuir surface area (m^2/g)	1956.8
[a] Pore volume (cm^3/g)	0.6674
[b] Pore size (Å)	18.54
Particle size [vol. weighted mean, (D [4,3]), µm]	19.14
Particle size [d(0.1), µm]	9.91
Particle size [d(0.5), µm]	24.89
Particle size [d(0.9), µm]	39.55

[a] Total pore volume of pores less than 1262 Å width.
[b] Adsorption average pore width (4 V/ A by BET).

1400 cm^{-1}, 1300 cm^{-1}, and 730 cm^{-1} and cellulosic fibers around 1100 cm^{-1}, 2700 cm^{-1}, and 3200 cm^{-1} (Fig. 5). Da Silva Pinto et al. [31] and Neufeld et al. [27] also reported that the Cu-BTC showed characteristic bands at the same wavelength. The deposition of the Cu-BTC on the cellulosic fibers by stirring or non-stirring resulted in an increase in bands intensity at 1700 cm^{-1}, 1447 cm^{-1}, 1343 cm^{-1}, and 729 cm^{-1}. The Cu-BTC showed COO − asymmetric bond, C − C stretches, COO − symmetric stretching, and C—H out-of-plane bending at 1644 cm^{-1}, 1447 cm^{-1}, 1343 cm^{-1}, and 729 cm^{-1}, respectively, which has also been reported by Da Silva Pinto et al. [31] and Neufeld et al. [27]. The cellulosic fibers showed characteristic bands around 1100 cm^{-1}, 2700 cm^{-1}, and 3200 cm^{-1} (Fig. 5). Stirring or non-stirring resulted in successful deposition of the Cu-BTC on the cellulosic fibers. It can be concluded that the Cu-BTC deposition increased the intensity of the characteristic peaks of the cellulosic fibers [27,31].

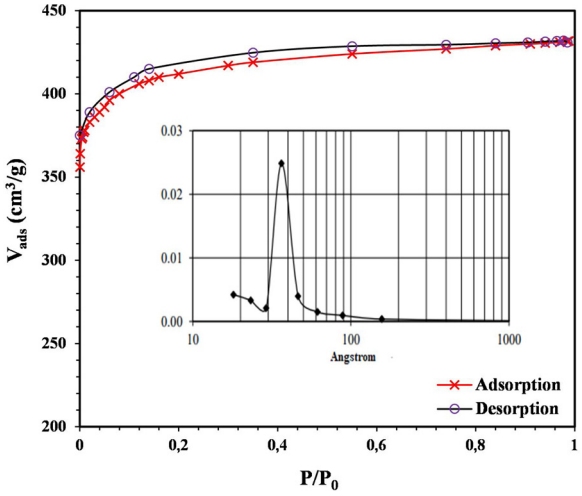

Fig. 3. BET isotherm of Cu-doped BTC (Cu-BTC).

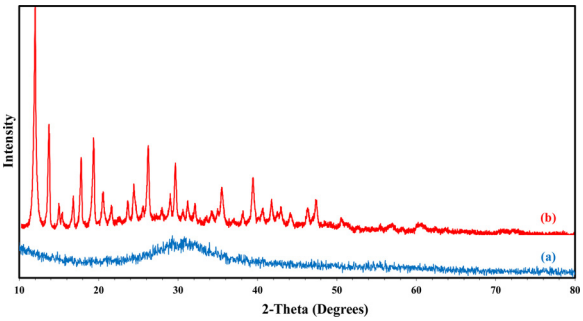

Fig. 4. XRD patterns of cellulosic woven waste (a) and Cu-doped BTC (Cu-BTC) (b).

The Cu-BTC particles were thermogravimetrically analyzed for thermal stability (Fig. 6). The TGA curve yielded an initial mass loss of 140–280 °C, corresponding to the loss of solvents from particle cages. Removal of those confined guest molecules may result in very large surface areas for the Cu-BTC. The Cu-BTC particles were thermally stable to 310 °C and then disrupted the cellulose structure, resulting in a sharp mass loss of 74.7 % at 280–490 °C. The result showed that the synthesized the Cu-BTC particles were able to retain their thermal stability up to about 280 °C [32].

A particle size analyzer was used to analyze the particle size

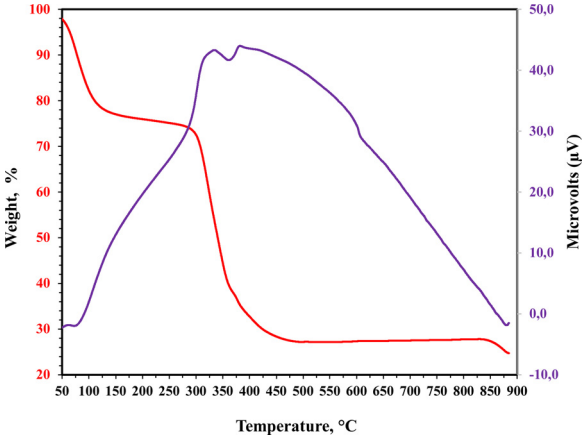

Fig. 6. TG/DTA-DSC diagram of Cu-doped BTC (Cu-BTC).

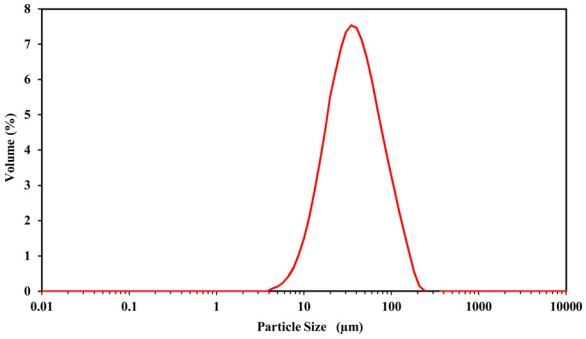

Fig. 7. Particle size diagram of Cu-doped BTC (Cu-BTC).

distribution of the Cu-BTC (Fig. 7). The result showed that the mean particle size of the synthesized the Cu-BTC was 32 μm (min 20 and max: 60) [33].

pH_{ZPC} was measured to examine the adsorption of methylene blue on the Cu-BTC [34]. The Cu-BTC had a pH_{ZPC} of 4.7, that is, the Cu-BTC had negative surface charges at pH higher than 4.7. This result indicated that there was a strong electrostatic interaction between the Cu-BTC and methylene blue when the solution pH was higher than pH_{ZPC} (Fig. 8).

3.2. The effect of pH

The Cu-BTC exhibited similar adsorption behavior (Fig. 9). The

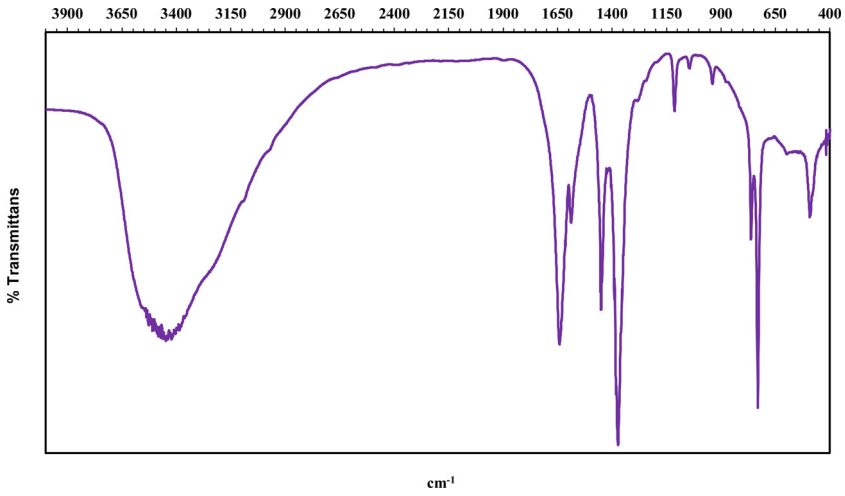

Fig. 5. FT-IR spectra of Cu-doped BTC (Cu-BTC).

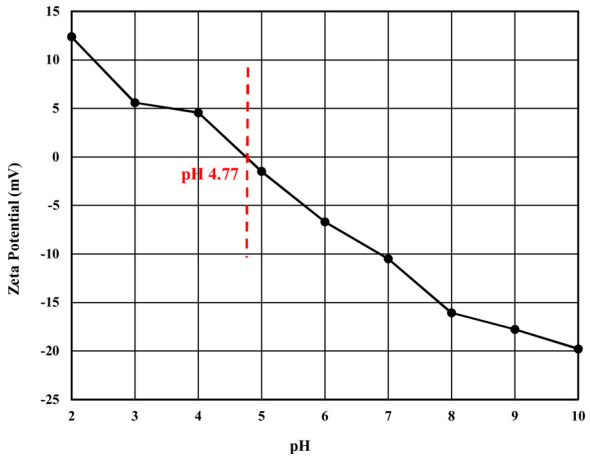

Fig. 8. pH_{zpc} diagram of Cu-doped BTC (Cu-BTC).

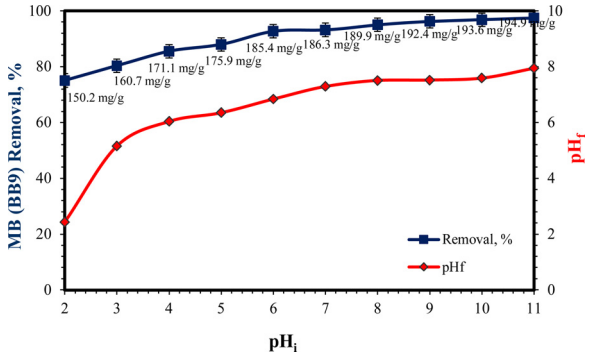

Fig. 9. Effect of pH on methylene blue (BB9) adsorption onto Cu-doped BTC (Cu-BTC).

removal rate of methylene blue by the Cu-BTC increased when the pH increased from 3 to 5 and then leveled off at around 84 % before reaching their highest peaks at pH = 11 (97.20 %). The variation in the methylene blue uptake due to solution pH corresponded to the pHpzc of the absorbent (Cu-BTC) and pKa of the absorbate (methylene blue). The Cu-BTC had a pH_{ZPC} of 4.7, while the methylene blue had a pKa of 6.9. The methylene blue was anionic, while the Cu-BTC were cationic at pH below 5. Removal rate increased consistently due to the electrostatic attraction between the Cu-BTC and the methylene blue. However, removal rate decreased slightly, suggesting that other adsorption mechanisms, such as ion-exchange, may be responsible for the adsorption behavior of the Cu-BTC at this stage. The Cu-BTC was cationic, and removal rate was stable at a pH of 2.5–4.5 due to the dominant van der Waals interaction [35–37]. The Cu-BTC was anionic at a pH of 4.5–9, resulting in an increase in removal rate due to electrostatic attraction. All absorbents were anionic, while methylene blue was cationic at pH above 9. All in all, the dye removal rate of the Cu-BTC rose significantly owing to electrostatic attraction.

3.3. Effect of ionic strength

The methylene blue removal rate increased slightly when 0.01 M NaCl solutions were added and reached maximum when 0.05 M NaCl solution was added (Fig. 10). Then it decreased with a decrease in NaCl concentrations. Relatively low NaCl concentrations may boost protonation and promote the dissociation of methylene blue molecules, thereby increasing removal rate. On the contrary, relatively high NaCl concentrations may suppress electrostatic interactions, resulting in reduced adsorption performance [38].

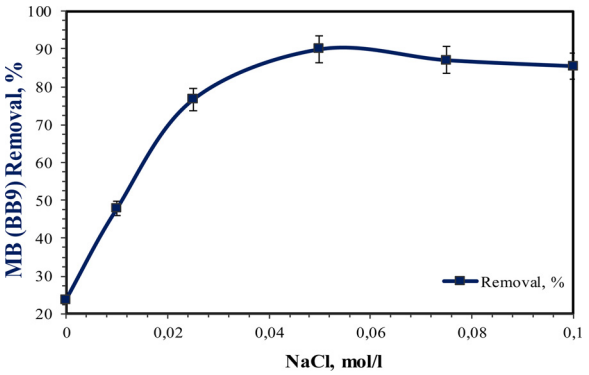

Fig. 10. Effect of ionic strength on methylene blue (BB9) adsorption onto Cu-doped BTC (Cu-BTC) [pH ~ 7].

3.4. Adsorption kinetics

The adsorption kinetics plays a key role in practice because it can be used to evaluate the yield of adsorption and the feasibility of scale-up operations [39–41]. Therefore, the experimental data were modeled using the Lagergren pseudo-first-order model, pseudo-second-order model, and interparticle diffusion to investigate the kinetics of methylene blue adsorption on the Cu-BTC. The kinetic equations are given in Table 2. The kinetic parameters and correlation coefficients (R^2) for each model are presented in Table 3. The kinetics of methylene blue adsorption on the Cu-BTC corresponded to the pseudo-second-order (Fig. 11). The effect of diffusion on the adsorption process was tested by applying the kinetic data to intra-particle diffusion model, of which the plot is shown in Table 3. Intra-particle diffusion constant parameters are tabulated in Table 3. According to Weber and Morris the intra-particle diffusion would be the rate limiting step if the plot of solute sorbed against the square root of the contact time yielded a straight line passing through the origin and the slope gives the rate constant K_{ipd}. In the present study, the linear plot of q_t vs $t^{0.5}$ did not pass through the origin. The relatively low R^2 values and the significant difference between the calculated and experimental adsorption capacity suggested that the pseudo-first-order model did not fit well to the adsorption process of the Cu-BTC. The pseudo-second-order model resulted in relative higher R^2 values (0.9927, 0.9934, and 0.9975 for 20 °C, 40 °C, and 60 °C) than the pseudo-first-order model (0.9303, 0.9255, and 0.9408 for 20 °C, 40 °C, and 60 °C). What is more, the experimental and calculated q_e values agreed well with each other. It can, therefore, be

Table 2
Adsorption kinetic models and equations.

Kinetic models	Equations	No
Pseudo-first order model	$\ln(q_e - q_t) = \ln q_e - k_1 t$ Plot: $\ln(q_e - q_t)$ vs.t k_1: Pseudo-first order kinetic rate coefficient (min^{-1})	(3)
Pseudo-second order model	$\frac{t}{q} = \frac{1}{k_2 q_e^2} + \frac{t}{q_e}$ Plot : t/q_t vs: t k: Pseudo-second order kinetic rate coefficient [(g/mg)/ min]	(4)
Intraparticle diffusion model	$q = k_i t^{1/2} + I$ Plot : q_t vs: $t^{1/2}$ k_{id}: Intraparticle diffusion rate coefficient [(mg/g)/ $min^{1/2}$] I: Intercept related to the thickness of boundary layer q_e: Adsorption capacity of the adsorbent at the equilibrium (mg/g) q_t: Adsorption capacity of the adsorbent at the time (t) (mg/g)	(5)

Table 3
Calculated model parameters and regression coefficients for kinetic (pseudo-first-order, pseudo-second-order and intraparticle diffusion) models for various temperatures.

Kinetic models	Parameters	Temperature		
		20°C	40°C	60°C
Pseudo	Equation	y = -0.0587x + 4.042	y = -0.00188x + 3.205	y = -0.0299x + 3.7038
First	k_1 (l/min)	0.0587	0.0188	0.0299
Order	q_{cal} (mg/g)	155.42	200.12	255.36
	R^2	0.9303	0.9255	0.9408
	X^2	10.8317	7.1740	6.2970
Pseudo	Equation	y = 0.0054x + 0.2297	y = 0.0068x + 0.1905	y = 0.0083x + 0.1171
Second	k_2 (g /(mg.min))	0.0054	0.0068	0.0083
Order	q_{cal} (mg/g)	195.15	237.86	294.14
	R^2	0.9927	0.9934	0.9975
	X^2	0.0087	0.0001	0.0059
Intra	Equation	y = 0.2219x + 20.55	y = 0.2514x + 30.78	y = 0.4757x + 45.72
Particle	k_{dif} (mg/(g. $min^{0.5}$))	0.2219	0.2514	0.4757
Diffusion	q_{cal} (mg/g)	17,955	22,078	27,772
	R^2	0.9814	0.9859	0.9865
	X^2	1.5907	1.3447	1.1332
q_{exp} (mg g^{-1})		196.45	238.01	295.46

concluded that the adsorption of methylene blue on the Cu-BTC followed the pseudo-second-order model. Table 3 indicates that the pseudo-second-order kinetic model with the highest R^2 values and smallest χ^2 values provided the best fit to the experimental data ([39–41].

3.5. Adsorption isotherm

Adsorption isotherms are used to describe the relationship between an adsorbate and an adsorbent at a constant temperature [39–41]. In this study, the adsorption data fitted well to the Langmuir isotherm model and the Freundlich isotherm model in linear form. The isotherm model equations used are given in Table 4. The isotherm parameters and correlation coefficients (R^2) for each model are presented in Table 5. The plot of the Langmuir isotherm model and Freundlich isotherm model are depicted in Fig. 12. The R^2 values of the Langmuir isotherm model (0.9951, 0.9990, and 0.9971 for 20 °C, 40 °C, and 60 °C) were relatively higher than those of the Freundlich isotherm model (0.9018, 0.9583, and 0.9362 for 20 °C, 40 °C, and 60 °C) (Table 5). This indicated that the experimental data better fit to the Langmuir isotherm model than to the Freundlich isotherm model. The estimated maximum adsorption capacity at 20 °C, 40 °C, and 60 °C was 189.12 ± 1.1 mg/g, 231.19 ± 0.9 mg/g, and 288.72 ± 1.4 mg/g, respectively, which were relatively larger than other raw leaf materials, such as Saraca asoca (90.9 mg/g) [42], Platanus orientalis (114.94 mg/g) [43], and fallen coconut leaves (112.35 mg/g) [44]. In conclusion, the Langmuir isotherm model confirmed that the adsorption of the methylene blue at 20 °C, 40 °C, and 60 °C was monolayer with identical adsorption affinities and activation energy over the homogeneous surface (Fig. 12a).

Table 4
Adsorption isotherm models and equations.

Isotherm models	Equations	No
Langmuir isotherm model	$\frac{C_e}{q_e} = \frac{1}{b.q_m} + \frac{C_e}{q_m}$ Plot : C_e/q_e vs. C_e b: Langmuir isotherm constant (L/mg) q_m: Maximum adsorption capacity (mg g^{-1})	(6)
Freundlich isotherm model	$lnq_e = \frac{1}{m} lnC_e + lnK_f$ Plot: lnq_e vs. lnC_e K_f: Freundlich isotherm constant related to adsorption capacity (mg/g).(L/mg)^n n: Freundlich isotherm constant related to adsorption intensity	(7)

Table 5
Calculated isotherm parameters for methylene blue(BB9) sorption by Cu-BTC.

Temperature °C	Langmuir			Freundlich		
	b (l/mg)	q_{max} (mg/g)	R^2	1/n	K_f ((mg/g^{-1})/(l/mg)$^{1/n}$)	R^2
20	32.3	189.12	0.9951	0.5515	13.661	0.9018
40	41.7	231.19	0.9990	0.4869	17.561	0.9583
60	50.6	288.72	0.9971	0.3948	22.839	0.9362

In addition, when non-linear isotherm (Fig. 12c) is examined, it can be stated that the methylene blue sorption of Cu-BTC has reached saturation within the operating conditions and is an L-type isotherm in

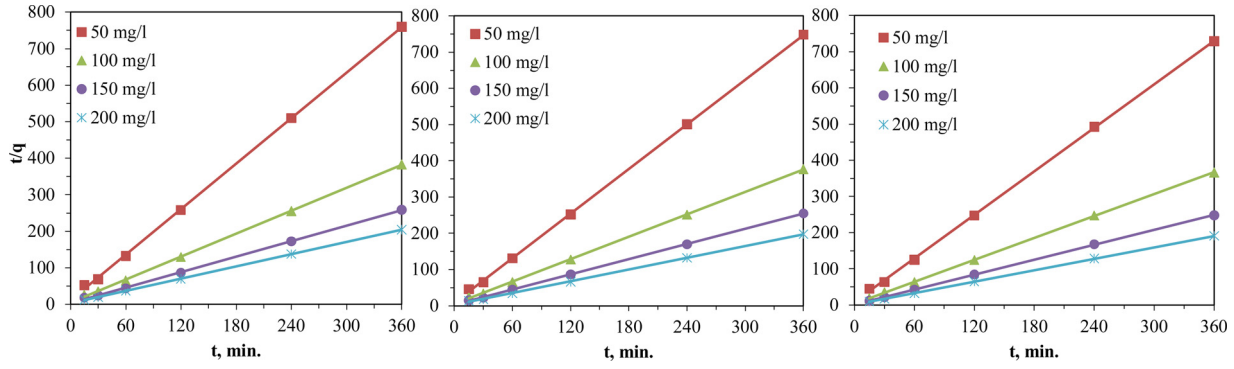

Fig. 11. Pseudo-second-order kinetic model plot for methylene blue (BB9) adsorption.

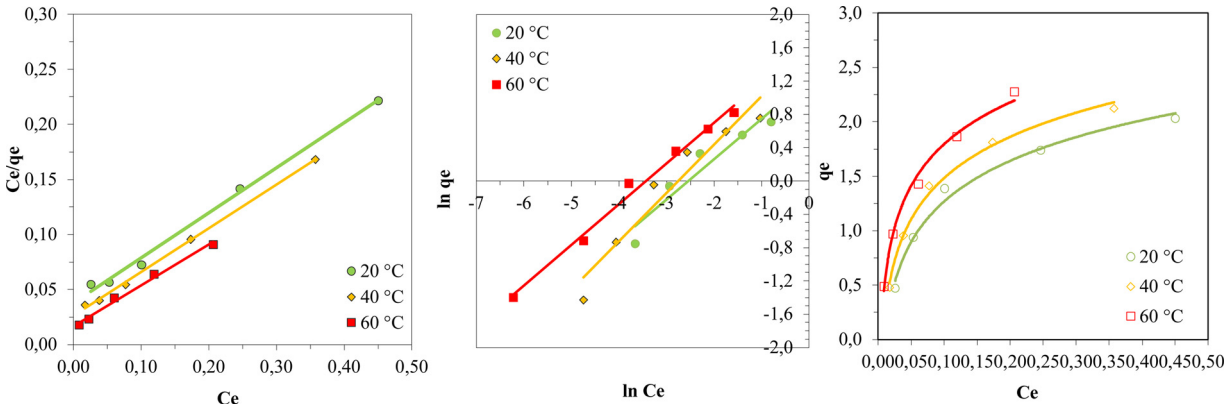

Fig. 12. Isotherm model plot for methylene blue (BB9) adsorption, (a) Langmuir isotherm model and (b) Freundlich isotherm model (c) Nonlinear sorption isotherm model.

the form of isotherm.

Numerous studies have used different materials to remove methylene blue from aqueous solutions and reported both kinetics and equilibrium operating parameters and capacities (Table 6). However, our results showed that the Cu-BTC had higher adsorption capacity than those materials, suggesting that it is a promising adsorbent that can be used to effectively remove methylene blue from aqueous solutions.

After experimental data are applied to the kinetic models, the speed constant of the most suitable model is considered to be the adsorption rate constant (k_{ad}). Activation energy is achieved by establishing a relationship between k_{ad} values and temperature at different concentrations and temperatures. To that end, the logarithm of the two lines is calculated (Eq. 8), and activation energy is obtained from the slope of the line drawn between lnk and 1/T.

$$k_{ad} = A(e^{-E_A/RT}) \quad (8)$$

where k_{ad} is the adsorption rate constant, A is the frequency factor, and E_a is the activation energy. For these parameters, units depend on the unit of the rate constant. Finally, activation energy can be calculated as kJ/mol.

E_A magnitude may provide a clue as to whether adsorption is of physical or chemical type. The former does not require a considerable amount of E_A because Van Der Waals forces, which are not higher than 1 kcal/mol (4.18 kJ/mol), are involved in the process. The latter, however, requires higher forces than does the former. Adsorption is of chemical type if the values of E_a are between 2 and 20 kcal/mol (8.4 and 83.7 kJ/mol) [35,40].

The experimental data fitted well to the simple II order kinetic model. The activation energy calculated from the Arrhenius equation for 50 − 200 mg/Lmethylene blue solutions was 18.03 ± 0.2kj/mol.

3.6. Thermodynamic studies

The three thermodynamic parameters, the Gibbs energy change

Table 6
Comparison of methylene blue (BB9) adsorption amounts in various adsorbents.

Adsorbent	q (mg/g)	References
Crystalline porous materials	315.2	[45]
MIL-100(Cr)	645.3	[46]
MOF-235	252.0	[47]
Papaya seeds	555.5	[48]
Activated carbon	400.0	[49]
Teak tree bark powder	333.3	[50]
Chitosan flakes	143.5	[51]
MOF compound	139.6	[52]
Hazelnut shell	38.2	[53]
CCuBTC composite MOF	288.72	This work

Table 7
Thermodynamic equations.

Isotherm models	Equations	No
Enthalpy (ΔH°)	$lnb = lnb_0 - \frac{\Delta H^\circ}{RT}$ Plot: lnb vs. 1/T	(9)
Free energy (ΔG°)	$ln\left(\frac{1}{b}\right) = \frac{\Delta G^\circ}{RT}$	(10)
Entropy (ΔS°)	$\Delta S^\circ = (\Delta H^\circ - \Delta G^\circ)/T$	(11)
	ΔG°, free energy exchange (kJ/mol); T is the absolute temperature (K) and R is the universal gas constant (8.314 J/molK). b can also be expressed in the following equation, including the terms ΔH° (kJ/mol) and ΔS° (kJ/molK), as a function of T	

Table 8
Thermodynamic parameters for methylene blue (BB9) sorption by Cu-BTC.

Temperature °C	ΔH (kj/mol)	ΔG (kj/mol)	ΔS (kj/mol.K)
20	9.12	−8.47	0.06001
40		−9.71	0.06015
60		−10.86	0.06000

(ΔG°), enthalpy change (ΔH°), and entropy change (ΔS°), were calculated using equations 9, 10, and 11 (Table 7). The value of ΔG° plays a key role in the spontaneity of adsorption. The ΔG° values decreased with an increase in temperature and were negative at all temperatures (Table 8), indicating that the adsorption process was favorable at 20 °C, 40 °C, and 60 °C. The values of ΔS° were positive at 20 °C, 40 °C, and 60 °C, suggesting increasing disorder of the interface during adsorption. The positive ΔS° values can be explained as follows: One adsorbate molecule is displaced by more than one water molecules during adsorption of dye, resulting in an increase in entropy [39–41]. The ΔH° values were positive at 20 °C, 40 °C, and 60 °C, meaning that the adsorption process was endothermic. Entropy, that is, irregularity decreased. This is because it becomes more regular with adsorbed agent accumulation/adhesion during adsorption.

3.7. Regeneration studies

It is not environmentally safe to dispose of adsorbents saturated with methylene blue. Therefore, different methods should be developed to regenerate and reuse adsorbents to reduce their environmental burden. This study investigated the regeneration performance of the Cu-BTC. The result of dilute acid (0.001 N HCl) regeneration is given in Table 9, indicating that the regenerated Cu-BTC had high adsorption capacity (about 159.48 ± 2.2 mg/g) after three consecutive dilute acid

Table 9
Regeneration studies for methylene blue (BB9) sorption by Cu-BTC.

Adsorpiton	MB (BB9) Removal, %	Sorption capcity mg/g
I	98.95	197.90
II	91.42	182.84
III	83.75	167.50
IV	79.74	159.48

treatments despite the reduction in regeneration efficiency from 91.42%–79.74%. This result indicates that dilute acid treatment can be used to improve the efficient and stable regeneration performance of the Cu-BTC [54,55].

3.8. Possible adsorption mechanism

A possible mechanism is provided to further explain that the Cu-BTC exhibits adsorption. The BET results showed that the Cu-BTC was in accordance with the adsorption event, which was confirmed by the adsorption application. Therefore, the average diameter of adsorption pore may also contribute to the adsorption performance of the Cu-BTC. According to the FTIR results, −OH, C═O were potential functional groups for the Cu-BTC interacting with methylene blue. These carboxyl acid groups were negative, which could combine with methylene blue dye^{+} via electrostatic attraction [56,57]. The pH results also confirmed that the adsorption process was mainly controlled by electrostatic force and had stable and efficient recycling performance during dilute acid (0.001 N HCl) treatment (Fig. 13). The methylene blue particles were decomposed during dilute acid (0.001 N HCl) treatment, resulting in more adsorption sites on the Cu-BTC surface. The π-π interactions may also enhance the regeneration efficiency of the Cu-BTC because it had unique surface layers interacting with dye molecules [58,59]. The higher the number of dilute acid (0.001 N HCl) treatments, the more stable the Cu-BTC structure, and thus, the more stable its regeneration performance.

3.9. Evaluation in terms of benefit and risk

Adsorption is an advanced physical/physicochemical treatment method based on the adsorption of pollutants on solids. The advantages of adsorption are that it is an efficient, easy-to-operate, and simple-design method that can either be used as a pretreatment or posttreatment for effective removal of pollutants from aqueous solutions. Adsorption is much easier and better at removing toxic pollutants from aqueous solutions than conventional biological wastewater treatments [60,61]. The Cu-BTC is an effective adsorbent used for removal of a wide range of pollutants (inorganic, organic, taste, odor, color, etc.) because it has high specific surface area, wide usability, and structural stability under acidic or basic conditions and at high temperatures [62]. Adsorption does not require too much effort. The disadvantages of adsorption are that it is disposable and sometimes causes turbidity [63], which we actually overcame by using it many times. Operating cost depends on how much the adsorbent and its regeneration cost. The disposal of adsorbents at their end of operational life also increases the cost. However, every treatment results in waste that should be disposed of. All these disadvantages can be done away with by imparting magnetic properties to the Cu-BTC. Adsorption be a very cost-effective method if the adsorbent is magnetized (no need for regeneration) or if new cost-effective adsorbents with active carbon properties (surface area, pore diameter, high stability, etc.) are manufactured. Adsorption does not pose a great risk because it is simple and requires no extreme operating conditions. However, operational accidents (spills and leakage of hazardous chemicals during disposal of adsorbents) may cause environmental and health problems. Landfill and incineration also increase the environmental burden of the disposal of adsorbents [64,65]. Every treatment results in waste that should be treated. Therefore, the key point is generating as little waste as possible after treatment. To achieve that, active adsorbents or magnetic adsorbents should be used.

4. Conclusion

The textile industry generates a large amount of cellulosic textile waste. In this study, a metal-organic framework Cu-doped BTC (Cu-BTC) was obtained from cellulosic textile waste and then used to remove methylene blue (BB9) from aqueous solutions. The equilibrium data agreed well with the Langmuir isotherm model. The Cu-BTC had a maximum monolayer adsorption capacity 189.12 ± 1.1 mg/g, 231.19 ± 0.9 mg/g, and 288.72 ± 1.4 at 20 °C, 40 °C, and 60 °C, respectively. The potential functional groups were mainly −OH and C═O, and electrostatic attraction played a key role in adsorption. The Cu-BTC regenerated by a dilute acid (0.001 N HCl) regeneration method performed well in three successive cycles without considerable loss of efficacy. Overall, the results indicate that the Cu-BTC is an effective adsorbent that can be used for dye removal from industrial wastewater and that repeated dilute acid (0.001 N HCl) regeneration methods can be used to regenerate adsorbents.

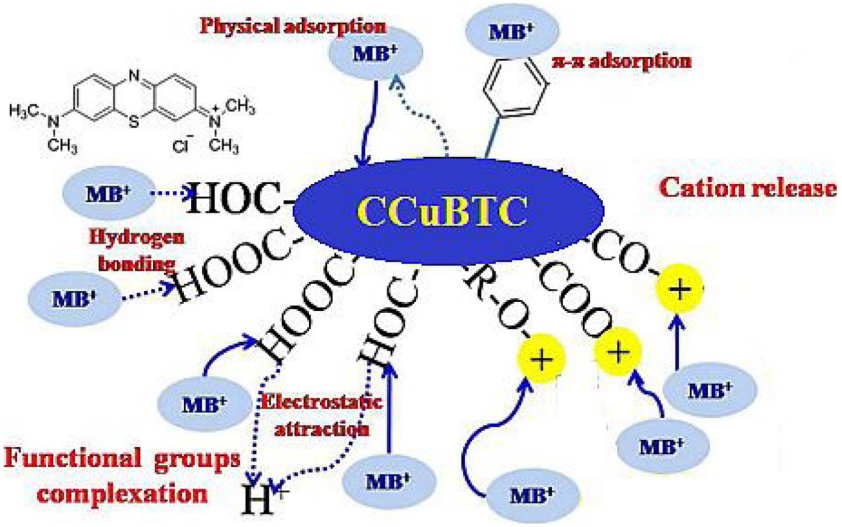

Fig. 13. Possible adsorption mechanism.

CRediT authorship contribution statement

Muhammet Ş.A. Eren: Conceptualization, Methodology, Software, Formal analysis. **Hasan Arslanoğlu:** Conceptualization, Methodology, Software, Formal analysis, Validation, Investigation, Writing - original draft, Writing - review & editing, Supervision. **Harun Çiftçi:** Methodology, Writing - original draft, Writing - review & editing.

Declaration of Competing Interest

The authors declare that there are no conflicts of interest.

References

[1] F.G.M. Borsagli, V.S. Ciminelli, C.L. Ladeira, D.J. Haas, A.P. Lage, H.S. Mansur, Multi-functional eco-friendly 3D scaffolds based on N-acyl thiolated chitosan for potential adsorption of methyl orange and antibacterial activity against Pseudomonas aeruginosa, J. Environ. Chem. Eng. 7 (5) (2019) 103286.

[2] L. Zhou, Q. Yu, Y. Cui, F. Xie, W. Li, Y. Li, M. Chen, Adsorption properties of activated carbon from reed with a high adsorption capacity, Ecol. Eng. 1 (2020).

[3] M. Fazlzadeh, R. Khosravi, A. Zarei, Green synthesis of zinc oxide nanoparticles using Peganum harmala seed extract, and loaded on Peganum harmala seed powdered activated carbon as new adsorbent for removal of Cr (VI) from aqueous solution, Ecol. Eng. 103 (2017) 180–190.

[4] A. Bianco Prevot, C. Baiocchi, M.C. Brussino, E. Pramauro, P. Savarino, V. Augugliaro, L. Palmisano, Photocatalytic degradation of acid blue 80 in aqueous solutions containing TiO_2 suspensions, Environ. Sci. Technol. 35 (5) (2001) 971–976.

[5] A. Yaraş, H. Arslanoğlu, Efficient removal of basic yellow 51 dye via carbonized paper mill sludge using sulfuric acid, Sigma J. Eng. Nat. Sci. 36 (3) (2018) 803–818.

[6] S.W. Won, H.J. Kim, S.H. Choi, B.W. Chung, K.J. Kim, Y.S. Yun, Performance, kinetics and equilibrium in biosorption of anionic dye Reactive Black 5 by the waste biomass of Corynebacterium glutamicum as a low-cost biosorbent, Chem. Eng. J. 121 (1) (2006) 37–43.

[7] H. Arslanoglu, F. Tumen, A study on cations and color removal from thin sugar juice by modified sugar beet pulp, J. Food Sci. Technol. 49 (3) (2012) 319–327.

[8] G.G. Sezer, O.Z. Yeşilel, O. Şahin, H. Arslanoğlu, İ. Erucar, Facile synthesis of 2D Zn (II) coordination polymer and its crystal structure, selective removal of methylene blue and molecular simulations, J. Mol. Struct. 1143 (2017) 355–361.

[9] H. Arslanoğlu, S. Kaya, F. Tümen, Cr (VI) adsorption on low-cost activated carbon developed from grape marc-vinasse mixture, Particul. Sci. Technol. (2019) 1–14.

[10] K. Kadirvelu, M. Palanival, R. Kalpana, S.J.B.T. Rajeswari, Activated carbon from an agricultural by-product, for the treatment of dyeing industry wastewater, Bioresour. Technol. 74 (3) (2000) 263–265.

[11] A. Yaraş, H. Arslanoğlu, Valorization of paper mill sludge as adsorbent in adsorption process of copper (II) ion from synthetic solution: kinetic, isotherm and thermodynamic studies, Arabian J. Sci. Eng. 43 (5) (2018) 2393–2402.

[12] C. Namasivayam, M.D. Kumar, K. Selvi, R.A. Begum, T. Vanathi, R.T. Yamuna, 'Waste'coir pith—a potential biomass for the treatment of dyeing wastewaters, Biomass Bioenergy 21 (6) (2001) 477–483.

[13] Y. Özdemir, M. Doğan, M. Alkan, Adsorption of cationic dyes from aqueous solutions by sepiolite, Microporous Mesoporous Mater. 96 (1-3) (2006) 419–427.

[14] K. Kadirvelu, M. Kavipriya, C. Karthika, M. Radhika, N. Vennilamani, S. Pattabhi, Utilization of various agricultural wastes for activated carbon preparation and application for the removal of dyes and metal ions from aqueous solutions, Bioresour. Technol. 87 (1) (2003) 129–132.

[15] H. Arslanoğlu, Direct and facile synthesis of highly porous low cost carbon from potassium-rich wine stone and their application for high-performance removal, J. Hazard. Mater. 374 (2019) 238–247.

[16] A.L. Abdullah, M.M. Salleh, M.S. Mazlina, M.J.M.M. Noor, M.R. Osman, R. Wagiran, S. Sobri, Azo dye removal by adsorption using waste biomass: sugarcane bagasse, Int. J. Eng. Technol. 2 (1) (2005) 8–13.

[17] S.E. Abdel-Aal, Y.H. Gad, A.M. Dessouki, Use of rice straw and radiation-modified maize starch/acrylonitrile in the treatment of wastewater, J. Hazard. Mater. 129 (1-3) (2006) 204–215.

[18] R. Gong, Y. Jin, F. Chen, J. Chen, Z. Liu, Enhanced malachite green removal from aqueous solution by citric acid modified rice straw, J. Hazard. Mater. 137 (2) (2006) 865–870.

[19] R. Gong, Y. Sun, J. Chen, H. Liu, C. Yang, Effect of chemical modification on dye adsorption capacity of peanut hull, Dye. Pigment. 67 (3) (2005) 175–181.

[20] C. Namasivayam, D. Sangeetha, Removal of molybdate from water by adsorption onto $ZnCl_2$ activated coir pith carbon, Bioresour. Technol. 97 (10) (2006) 1194–1200.

[21] A.E. Ofomaja, Kinetics and mechanism of methylene blue sorption onto palm kernel fibre, Process Biochem. 42 (1) (2007) 16–24.

[22] O. Hamdaoui, Batch study of liquid-phase adsorption of methylene blue using cedar sawdust and crushed brick, J. Hazard. Mater. 135 (1-3) (2006) 264–273.

[23] J.F. Osma, V. Saravia, J.L. Toca-Herrera, S.R. Couto, Sunflower seed shells: a novel and effective low-cost adsorbent for the removal of the diazo dye Reactive Black 5 from aqueous solutions, J. Hazard. Mater. 147 (3) (2007) 900–905.

[24] P. Küsgens, S. Siegle, S. Kaskel, Crystal growth of the metal—organic framework Cu3 (BTC) 2 on the surface of pulp fibers, Adv. Eng. Mater. 11 (1-2) (2009) 93–95.

[25] R.M. Abdelhameed, H.E. Emam, J. Rocha, A.M. Silva, The Cu-BTC metal-organic framework natural fabric composites for fuel purification, Fuel Process. Technol. 159 (2017) 306–312.

[26] P. Falcaro, R. Ricco, A. Yazdi, I. Imaz, S. Furukawa, D. Maspoch, C.J. Doonan, Application of metal and metal oxide nanoparticles@ MOFs, Coord. Chem. Rev. 307 (2016) 237–254.

[27] M.J. Neufeld, J.L. Harding, M.M. Reynolds, Immobilization of metal–organic framework copper (II) benzene-1, 3, 5-tricarboxylate (CuBTC) onto cotton fabric as a nitric oxide release catalyst, ACS Appl. Mater. Interfaces 7 (48) (2015) 26742–26750.

[28] K. Pirzadeh, A.A. Ghoreyshi, M. Rahimnejad, M. Mohammadi, Electrochemical synthesis, characterization and application of a microstructure Cu3(BTC)2 metal organic framework for CO_2 and CH_4 separation, Korean J. Chem. Eng. 35 (4) (2018) 974–983.

[29] G.W. Peterson, D.K. Britt, D.T. Sun, J.J. Mahle, M. Browe, T. Demasky, J.A. Rossin, Multifunctional purification and sensing of toxic hydride gases by CuBTC metal–organic framework, Ind. Eng. Chem. Res. 54 (14) (2015) 3626–3633.

[30] N. Motakef-Kazemi, S.A. Shojaosadati, A. Morsali, In situ synthesis of a drug-loaded MOF at room temperature, Microporous Mesoporous Mater. 186 (2014) 73–79.

[31] M. Da Silva Pinto, C.A. Sierra-Avila, J.P. Hinestroza, In situ synthesis of a Cu-BTC metal–organic framework (MOF 199) onto cellulosic fibrous substrates: cotton, Cellulose 19 (5) (2012) 1771–1779.

[32] A. Modrow, D. Zargarani, R. Herges, N. Stock, The first porous MOF with photoswitchable linker molecules, Dalton Trans. 40 (16) (2011) 4217–4222.

[33] R.S. Kumar, S.S. Kumar, M.A. Kulandainathan, Efficient electrosynthesis of highly active Cu3 (BTC) 2-MOF and its catalytic application to chemical reduction, Microporous Mesoporous Mater. 168 (2013) 57–64.

[34] M. Ravanipour, R. Kafaei, M. Keshtkar, S. Tajalli, N. Mirzaei, B. Ramavandi, Fluoride ion adsorption onto palm stone: optimization through response surface methodology, isotherm, and adsorbent characteristics data, Data Brief 12 (2017) 471–479.

[35] H. Arslanoglu, Adsorption of micronutrient metal ion onto struvite to prepare slow release multielement fertilizer: copper (II) doped-struvite, Chemosphere 217 (2019) 393–401.

[36] H. Ciftci, Removal and preconcentration of cadmium on polystyrene-graft-ethylmethacrylate copolymer, Environ. Eng. Manage. J. 13 (3) (2014) 635–642.

[37] H. Arslanoglu, Removal of Cu (II) from aqueous solutions by using marble waste, Pamukkale Univ, J. Eng. Sci. 23 (7) (2017) 877–886.

[38] Y. Wu, H. Pang, W. Yao, X. Wang, S. Yu, Z. Yu, X. Wang, Synthesis of rod-like metal-organic framework (MOF-5) nanomaterial for efficient removal of U (VI): batch experiments and spectroscopy study, Sci. Bull. 63 (13) (2018) 831–839.

[39] S. Lin, Z. Song, G. Che, A. Ren, P. Li, C. Liu, J. Zhang, Adsorption behavior of metal–organic frameworks for methylene blue from aqueous solution, Microporous Mesoporous Mater. 193 (2014) 27–34.

[40] H. Arslanoğlu, R. Orhan, M.D. Turan, Application of response surface methodology for the optimization of copper removal from aqueous solution by activated carbon prepared using waste polyurethane, Anal. Lett. 53 (9) (2019) 1343–1365.

[41] A. Beheshti, K. Nozarian, N. Ghamari, P. Mayer, H. Motamedi, Selective high capacity adsorption of Congo red, luminescence and antibacterial assessment of two new cadmium (II) coordination polymers, J. Solid State Chem. 258 (2018) 618–627.

[42] N. Gupta, A.K. Kushwaha, M.C. Chattopadhyaya, Adsorption studies of cationic dyes onto Ashoka (Saraca asoca) leaf powder, J. Taiwan Inst. Chem. Eng. 43 (4) (2012) 604–613.

[43] M. Peydayesh, A. Rahbar-Kelishami, Adsorption of methylene blue onto Platanus orientalis leaf powder: kinetic, equilibrium and thermodynamic studies, J. Ind. Eng. Chem. 21 (2015) 1014–1019.

[44] A.H. Jawad, R.A. Rashid, R.M. Mahmuod, M.A.M. Ishak, N.N. Kasim, K. Ismail, Adsorption of methylene blue onto coconut (Cocos nucifera) leaf: optimization, isotherm and kinetic studies, Desalin. Water Treat. 57 (19) (2016) 8839–8853.

[45] T.F. Willems, C.H. Rycroft, M. Kazi, J.C. Meza, M. Haranczyk, Algorithms and tools for high-throughput geometry-based analysis of crystalline porous materials, Microporous Mesoporous Mater. 149 (1) (2012) 134–141.

[46] M. Tong, D. Liu, Q. Yang, S. Devautour-Vinot, G. Maurin, C. Zhong, Influence of framework metal ions on the dye capture behavior of MIL-100 (Fe, Cr) MOF type solids, J. Mater. Chem. A 1 (30) (2013) 8534–8537.

[47] E. Haque, J.W. Jun, S.H. Jhung, Adsorptive removal of methyl orange and methylene blue from aqueous solution with a metal-organic framework material, iron terephthalate (MOF-235), J. Hazard. Mater. 185 (1) (2011) 507–511.

[48] B.H. Hameed, Evaluation of papaya seeds as a novel non-conventional low-cost adsorbent for removal of methylene blue, J. Hazard. Mater. 162 (2-3) (2009) 939–944.

[49] K.V. Kumar, S. Sivanesan, Equilibrium data, isotherm parameters and process design for partial and complete isotherm of methylene blue onto activated carbon, J. Hazard. Mater. 134 (1-3) (2006) 237–244.

[50] S. Patil, S. Renukdas, N. Patel, Removal of methylene blue, a basic dye from aqueous solutions by adsorption using teak tree (Tectona grandis) bark powder, Int. J. Environ. Sci. 1 (5) (2011) 711–726.

[51] F. Marrakchi, M.J. Ahmed, W.A. Khanday, M. Asif, B.H. Hameed, Mesoporous-activated carbon prepared from chitosan flakes via single-step sodium hydroxide activation for the adsorption of methylene blue, Int. J. Biol. Macromol. 98 (2017) 233–239.

[52] G.G. Sezer, M. Arıcı, I. Erucar, O.Z. Yeşilel, H.U. Özel, B.T. Gemici, H. Erer, Zinc (II) and cadmium (II) coordination polymers containing phenylenediacetate and 4, 4′-azobis (pyridine) ligands: syntheses, structures, dye adsorption properties and molecular dynamics simulations, J. Solid State Chem. 255 (2017) 89–96.

[53] M. Doğan, H. Abak, M. Alkan, Biosorption of methylene blue from aqueous solutions by hazelnut shells: equilibrium, parameters and isotherms, Water Air Soil Pollut. 192 (1-4) (2008) 141–153.
[54] M.R. Awual, A. Jyo, T. Ihara, N. Seko, M. Tamada, K.T. Lim, Enhanced trace phosphate removal from water by zirconium (IV) loaded fibrous adsorbent, Water Res. 45 (15) (2011) 4592–4600.
[55] R.K. Gautam, A. Mudhoo, G. Lofrano, M.C. Chattopadhyaya, Biomass-derived biosorbents for metal ions sequestration: adsorbent modification and activation methods and adsorbent regeneration, J. Environ. Chem. Eng. 2 (1) (2014) 239–259.
[56] E. Errais, J. Duplay, M. Elhabiri, M. Khodja, R. Ocampo, R. Baltenweck-Guyot, F. Darragi, Anionic RR120 dye adsorption onto raw clay: surface properties and adsorption mechanism, Colloids Surf. A Physicochem. Eng. Asp. 403 (2012) 69–78.
[57] K.B. Tan, M. Vakili, B.A. Horri, P.E. Poh, A.Z. Abdullah, B. Salamatinia, Adsorption of dyes by nanomaterials: recent developments and adsorption mechanisms, Sep. Pur. Technol. 150 (2015) 229–242.
[58] M. Doğan, M. Alkan, A. Türkyilmaz, Y. Özdemir, Kinetics and mechanism of removal of methylene blue by adsorption onto perlite, J. Hazard. Mater. 109 (1-3) (2004) 141–148.
[59] N.A. Travlou, G.Z. Kyzas, N.K. Lazaridis, E.A. Deliyanni, Graphite oxide/chitosan composite for reactive dye removal, Chem. Eng. J. 217 (2013) 256–265.
[60] I. Oller, S. Malato, J. Sánchez-Pérez, Combination of advanced oxidation processes and biological treatments for wastewater decontamination—a review, Sci. Total Environ. 409 (20) (2011) 4141–4166.
[61] A. Yaraş, H. Arslanoğlu, Utilization of paper mill sludge for removal of cationic textile dyes from aqueous solutions, Sep. Sci. Technol. 54 (16) (2019) 2555–2566.
[62] A. Mittal, M. Teotia, R.K. Soni, J. Mittal, Applications of egg shell and egg shell membrane as adsorbents: a review, J. Mol. Liq. 223 (2016) 376–387.
[63] E. Rott, M. Nouri, C. Meyer, R. Minke, M. Schneider, K. Mandel, A. Drenkova-Tuhtan, Removal of phosphonates from synthetic and industrial wastewater with reusable magnetic adsorbent particles, Water Res. 145 (2018) 608–617.
[64] P.S. Kulkarni, J.G. Crespo, C.A. Afonso, Dioxins sources and current remediation technologies—a review, Environ. Int. 34 (1) (2008) 139–153.
[65] E.C. Souza, T.C. Vessoni-Penna, R.P. de Souza Oliveira, Biosurfactant-enhanced hydrocarbon bioremediation: an overview, Int. Biodeter. Biodegrad. 89 (2014) 88–94.